Ratiometric control of two microbial populations in a dual chamber bioreactor

Sara Maria Brancato, Davide Salzano, Davide Fiore, Giovanni Russo, Mario di Bernardo

***Abstract*— Ensuring stable coexistence between different species in microbial consortia is a challenging problem, especially when the species are not complementary, i.e. one species always outgrowing the other when left uncontrolled. Here, we present a novel control architecture based on the use of two bioreactors in which the slower species is separately grown and can be added to the main mixing chamber. After analyzing the open-loop dynamics of this multicellular system, we present a switching feedback strategy that, by controlling the dilution rates, guarantees robust regulation of both density and composition. We validate in silico the effectiveness and robustness of the proposed approach using models parameterized onto real experiments. The numerical results illustrate the potential applicability of our approach across diverse microbial strains without the need for any genetic modifications.**

I. INTRODUCTION

Microbes in nature are often organized in consortia comprising multiple interacting populations that cooperate to achieve a common goal [1]. This self-organization increases the survival fitness of the community and, by specialization and division of labor, reduces the burden on each population while increasing the overall efficiency of the consortium [2]. Over the past decade the translation of these advantages to synthetically engineered biological systems has attracted increasing interest [3] as it is an effective solution for the efficient production of complex chemical compounds [4]–[6].

In addition to the design of the phenotype of each population, the realization of functional microbial consortia requires stable, long-term coexistence between the different populations present in the consortium. This task is challenging to achieve as each population, engineered with different genetic regulatory networks, is burdened by a different metabolic load, resulting in heterogeneous growth rates. Left uncontrolled, this imbalance will ultimately lead to the extinction of one or more populations, disrupting the proper functioning of the consortium. Thus, the key issue of regulating the microbial community's composition, known as composition, or ratiometric, control, is essential for creating consortia capable of reliably performing the desired function [7].

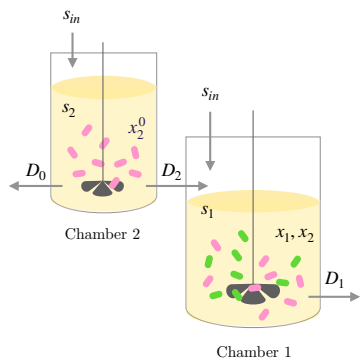

Fig. 1. Schematic representation of the two-reactor architecture. The slower species (species 2, in pink) is grown separately in chamber 2 and added at rate D_2 in chamber 1, where it is mixed with species 1 (in green). Species 2 is regulated at the desired concentration $\bar{x}_2^0$ in chamber 2 by means of the dilution rate D_0. The dilution rate D_1 is used in combination with D_2 to keep the two species at the desired concentrations in chamber 1.

A promising scalable approach to the co-culture of multiple bacterial populations is to use single or multiple bioreactors to control the overall density of the consortium, as well as its composition. Different solutions have been proposed in the literature to solve this problem within a single bioreactor. For example, in [8] a deep reinforcement learning algorithm was used to decide the composition of the growth media to guarantee the coexistence of two microbial populations feeding on different substrates. Alternatively, in [9], [10] it is shown that, by using the dilution rate as a control input, it is possible to robustly enable coexistence between two complementary strains. Both approaches rely on the assumption that it is possible to change the growth conditions so as to make either population dominant in terms of growth rate. However, it is not always possible to create such conditions since the growth properties, determined by the amount of cellular resources used up to a given time, might remain fixed. In the case of co-cultures, this means that the population using up more resources will always grow slower and will eventually become extinct. In a single bioreactor,

Davide Salzano and Davide Fiore contributed equally to this work. Corresponding author: Mario di Bernardo.

Sara Maria Brancato and Mario di Bernardo are with the Department of Electrical Engineering and Information Technology, University of Naples Federico II, Via Claudio 21, 80125 Naples, Italy (email: saramaria.brancato@unina.it). Mario di Bernardo is also with the SSM - School for Advanced Studies, Naples, Italy (email: mario.dibernardo@unina.it). Davide Salzano is with the SSM - School for Advanced Studies, Naples, Italy (email: davide.salzano@unina.it). Giovanni Russo is with the Department of Information Engineering, Electrical Engineering and Applied Mathematics, University of Salerno, 84084, Fisciano, Italy (email: giovarusso@unisa.it). Davide Fiore is with the Department of Mathematics and Applications "R. Caccioppoli", University of Naples Federico II, Via Cintia, Monte S.Angelo, 80126 Naples, Italy (email: davide.fiore@unina.it).

The authors like to express our sincere gratitude to the TIGEM (Telethon Institute of Genetics and Medicine) laboratory for their invaluable support and collaboration throughout this research project. DF and GR wish to acknowledge financial support by the European Union - Next Generation EU, under PRIN 2022 PNRR, Project "Control of smart microbial communities for wastewater treatment". MdB wishes to acknowledge financial support by the Italian Ministry of Health under PNRR PNC, Project "Digital Health Solutions in Community Medicine (DHEAL-COM)" – Project Code PNC-E3-2022-23683267 PNC – HLS – DH.

this cannot be avoided even when using a sophisticated feedback control action due to the competitive exclusion principle [11], which from a dynamical systems standpoint translates into the system being uncontrollable. Therefore, a more general methodology is needed to guarantee long-term coexistence of different microbial species in a bioreactor.

In this Letter, we propose an experimental platform endowed with a control strategy for robust regulation of both the density and the composition of a microbial consortium made of two non-complementary strains (one population persistently growing faster than the other). Specifically, we will use two communicating bioreactors (turbidostat) (see Fig. 1), where the former hosts a mixture of both populations, while the latter is used as a reservoir where the slower population is grown alone. By using as control input the dilution rate D_1 (inlet volumetric flow/volume) associated with fresh media in the first reactor in combination with the dilution rate D_2, at which the slower population from the reservoir (kept at a reference density therein by means of the dilution rate D_0) is added to the mixing chamber, our strategy is able to guarantee the coexistence between the two populations at a desired ratio.

In what follows, after introducing the mathematical model describing the growth dynamics of each population within every reactor and analyzing its asymptotic behavior, we propose both an open-loop and a closed-loop controller that are able to regulate the density of the consortium, as well as its composition. Finally, we numerically validate the performance and robustness properties of the control strategies on a model parametrized on real experimental data collected using two Chi.Bio turbidostats [12]. The proposed approach offers the advantage of being applicable to a wide range of strains, provided they grow on the same substrate, without requiring genetic engineering interventions.

II. Mathematical Model

We consider two microbial species growing as a continuous culture in a chemostat (labeled as chamber 1 in Fig. 1), with a reservoir (chamber 2 in Fig. 1) in which one species grows separately . The two species are assumed to be independent, that is, they grow on the same substrate but they do not directly condition the growth rate of each other. The mathematical model of the former chemostat with two species and two inputs can be expressed as

$$\begin{cases} \dot{x}_1 = \mu_1(s_1)x_1 - D_1(t)x_1 - D_2(t)x_1 \\ \dot{x}_2 = \mu_2(s_1)x_2 - D_1(t)x_2 + D_2(t)(x_2^0 - x_2) \\ \dot{s}_1 = -\frac{1}{Y_1}\mu_1(s_1)x_1 - \frac{1}{Y_2}\mu_2(s_1)x_2 \\ \qquad + D_1(t)(s_{\text{in}} - s_1) + D_2(t)(s_2 - s_1) \end{cases}, \quad (1)$$

where the variables $x_1, x_2 \in \mathbb{R}_{\geq 0}$ and $s_1, s_2 \in [0, s_{\text{in}}]$ denote the concentrations of the biomass of species 1 and 2 and of the substrate in chamber 1 and 2, respectively, while the mathematical model of the reservoir (chamber 2) is given by

$$\begin{cases} \dot{x}_2^0 = (\mu_2(s_2) - D_0(t) - D_2(t))x_2^0 \\ \dot{s}_2 = -\frac{1}{Y_2}\mu_2(s_2)x_2^0 + (D_0(t) + D_2(t))(s_{\text{in}} - s_2) \end{cases}, \quad (2)$$

where $x_2^0 \in \mathbb{R}_{\geq 0}$ denotes the concentration of the biomass of the species 2 in the chamber 2. Moreover, $\mu_i(\cdot)$, $i = 1, 2$, are the growth rates of species i (defined below), Y_i is the yield coefficient, assumed without loss of generality to be unitary for both species, and s_{in} is the concentration of the substrate in the inlet flows. The control inputs D_i are the dilution rates defined as the ratio between the inlet flow rate and the culture volume. Specifically, the control inputs $D_1(t) : \mathbb{R}_{\geq 0} \mapsto [D_{1,\min}, D_{1,\max}]$, with $D_{1,\min} > 0$, and $D_0(t) : \mathbb{R}_{\geq 0} \mapsto [D_{0,\min}, D_{1,\max}]$, with $D_{0,\min} > 0$, dilute the concentrations in chambers 1 and 2, respectively, by injecting fresh substrate at concentration s_{in}, while the input $D_2(t) : \mathbb{R}_{\geq 0} \mapsto [0, D_{2,\max}]$ is the dilution rate due to the inlet flow of media from chamber 2 to chamber 1. The dilution rates are assumed to be the same for both species, that is, the culture is well-mixed and mortality and attachment of the bacteria are neglected [10].

The dynamics of systems (1)-(2) is characterized by the growth rate functions $\mu_i(\cdot) : [0, s_{\text{in}}] \mapsto \mathbb{R}_{\geq 0}$, that are typically assumed to be differentiable, strictly increasing, and such that $\mu_i(0) = 0$, for $i = 1, 2$ [13]. When the growth functions intersect more than once, it is possible to design some control input $D_1(t)$ (setting $D_2 = 0$) such that both species survive [9], [10], [14]. On the contrary, when it holds that

$$\mu_1(s) > \mu_2(s), \quad \text{for all } s \in (0, s_{\text{in}}], \quad (3)$$

the growth functions intersect only at 0 and the two species are said to be non-complementary [10], i.e. one species always outgrowing the other. Therefore, in this condition, from the Competitive Exclusion Principle (CEP) [15], it follows that when inflow from the additional reservoir is not available, i.e., $D_2 = 0$, no control input $D_1(t)$ exists such that more than one strain survives at steady state. However, in our architecture coexistence is still made possible by injecting into the chemostat (chamber 1) some *extra* biomass of the slower species taken from the reservoir (chamber 2) by means of the additional control input $D_2(t)$.

In the rest of this paper, we consider growth functions of Monod's type [13], that is,

$$\mu_i(s) := \frac{\mu_i^* s}{k_i + s}, \quad i = 1, 2, \quad (4)$$

where μ_i^* and k_i are positive constants.

A. Dynamics

Under the assumption that the sum of the control inputs $D_0(t)$ and $D_2(t)$ is persistently exciting, that is, such that $\int_0^{+\infty}(D_0(\tau) + D_2(\tau))d\tau = +\infty$, the solutions of system (2) are attracted to the invariant subspace $\mathcal{S}_0 := \{(x_2^0, s_2) : x_2^0 + s_2 = s_{\text{in}}\}$, see [10] for further details. Thus, if the initial condition $x_2^0(0)$ belongs to $\mathcal{S}_0$, the dynamics of (2) on $\mathcal{S}_0$ can be reduced to:

$$\dot{x}_2^0 = (\mu_2(s_2) - D_0(t) - D_2(t))x_2^0. \quad (5)$$

Likewise, under the assumption that the sum of $D_1(t)$ and $D_2(t)$ is persistently exciting, the solutions of system (1) are attracted to the invariant subspace $\mathcal{S} := \{(x_1, x_2, s_1) :$

$x_1 + x_2 + s_1 = s_{\rm in}\}$ and solutions rooted therein can be described by the reduced order model:

$$\begin{cases} \dot{x}_1 = (\mu_1(s_1) - D_1(t) - D_2(t))x_1 \\ \dot{x}_2 = (\mu_2(s_1) - D_1(t) - D_2(t))x_2 + D_2(t)x_2^0 \end{cases}, \quad (6)$$

defined on the invariant set $\mathcal{S}_r := \{(x_1, x_2) \in \mathbb{R}^2_{\geq 0} : x_1 + x_2 \leq s_{\rm in}\}$.

Depending on the value of $(D_0 + D_2)$, system (5) can have one or two equilibria. One equilibrium is always at 0, while the other is $\bar{x}_2^0 = s_{\rm in} - \bar{s}_2$, with

$$\bar{s}_2 = \frac{k_2(D_0 + D_2)}{\mu_2^* - (D_0 + D_2)}. \quad (7)$$

The point $\bar{x}_2^0$ is admissible and stable for $0 < (D_0 + D_2) < \mu_2(s_{\rm in})$, and it becomes non-admissible, exchanging its stability with the point at the origin, when $(D_0+D_2) = \mu_2(s_{\rm in})$, through a transcritical bifurcation.

System (6) has a richer dynamics depending on the values of D_1 and D_2. The most interesting scenario is when $D_2 > 0$. In this case, if $D_1 + D_2 < \mu_1(s_{\rm in})$ there exists a stable equilibrium point in $\mathcal{S}_r$ such that both species coexist. This point is located at the intersection between the x_1-nullcline ($\dot{x}_1 = 0$)

$$x_2 = -x_1 + s_{\rm in} - \frac{k_1(D_1 + D_2)}{\mu_1^* - (D_1 + D_2)}, \quad (8)$$

and the x_2-nullcline ($\dot{x}_2 = 0$)

$$x_2 = \frac{D_2 x_2^0}{(D_1 + D_2) - \mu_2(s_{\rm in} - x_1 - x_2)}, \quad (9)$$

Moreover, there exists another equilibrium point, that is unstable, lying on the x_2-axis ($x_1 = 0$) at the intersection with (9). When $D_1 + D_2$ is above a critical value, the coexistence point collides with the unstable point on the x_2-axis, exchanging stability in a transcritical bifurcation, and ceases to be admissible. At this point only species 2 survives, because the total dilution rate in the bioreactor is too high for species 1 to survive. However, note that the complete extinction of species 1 is not possible in practice, as experimentally some cells will not be flushed out.

The other two less interesting scenarios occur when (i) $D_1 \approx 0$ and (ii) $D_2 = 0$. In the first case ($D_1 \approx 0$), the dynamics is similar to the previous case, that is, there exists a stable equilibrium point associated to coexistence whose position depends only on D_2. However, when $D_2 > \mu_1(s_{\rm in})$, that is, the dilution rate from the reservoir is higher than the maximum growth rate of species 1, the faster species is flushed-out from the bioreactor ($\bar{x}_1 \approx 0$) and as D_2 increases the concentration of species 2 reaches asymptotically the same value as in the reservoir (i.e., $\bar{x}_2 \approx x_2^0$). In the second case ($D_2 = 0$), model (6) becomes the same model described in [9], and as D_1 varies from 0 to $D_{1,\max} > \mu_1(s_{\rm in})$ we retrieve the same dynamics depicted in the phase portraits shown in Fig. 2 from [9] (namely cases I, IV, V, VI). The case $D_1 = D_2 = 0$, for which the attractive equilibrium set $\mathcal{E}_0 := \{(x_1, x_2) \in \mathcal{S}_r : x_2 = -x_1 + s_{\rm in}\}$ exists, is excluded from the analysis because it corresponds to the biomass being in starvation and therefore it is not an admissible working condition in continuous culture (see case I in Fig. 2 from [9]).

III. Control Problem

Given the two-chambers bioreactor architecture, depicted in Fig. 1, with two *non-complementary* microbial species, i.e. such that condition (3) holds, whose mathematical model and dynamics have been described in Sec. II, our control objective is to control the dilution rates such that at steady state the two species coexist and their concentrations are regulated at a desired ratio. That is, we want to solve the following problem.

Control problem: Design some control inputs $D_0(t)$, $D_1(t)$, and $D_2(t)$ for system (5)-(6), under condition (3), such that:

1) *coexistence* of the two species is guaranteed for all time, that is, $x_i(t) > x_{i,\min}$, $\forall t > 0$, $i = 1, 2$, where $x_{i,\min} > 0$ is some safety value to avoid extinction of species i;
2) the *total biomass* is regulated to a desired value to guarantee efficient utilization of the resources, that is,
$$x_1(t) + x_2(t) = OD_{\rm d}, \quad \text{as} \quad t \to +\infty, \quad (10)$$
where $OD_{\rm d}$ is the desired optical density in chamber 1, assumed for the sake of simplicity to be an exact proxy of the total biomass therein;
3) the *ratio* x_2/x_1 between the concentration of the two species in the chamber 1 is robustly regulated at steady state to a desired value $r_{\rm d}$, that is,
$$x_2(t) = r_{\rm d} \cdot x_1(t), \quad \text{as} \quad t \to +\infty. \quad (11)$$

Notice that the above control problem corresponds to requiring that all solutions of system (5)-(6), starting from any initial conditions in $\mathcal{S}_0 \cup \mathcal{S}_r$, converge to the point of intersection between the two lines defined in (10) and (11) (Fig. 2), that is, to the point

$$x_{\rm d} := \left(\frac{OD_{\rm d}}{1 + r_{\rm d}}, r_{\rm d} \frac{OD_{\rm d}}{1 + r_{\rm d}} \right). \quad (12)$$

In the following, we assume that the concentrations x_1, x_2 and x_2^0 are either directly or indirectly measurable, for example via fluorescent reporters or state observers.

IV. Open-loop control

A simple open-loop controller that solves the control problem described above can be designed by exploiting the dynamics of the system described in Sec. II-A, that is, by choosing constant values $\bar{D}_0$, $\bar{D}_1$ and $\bar{D}_2$ so as to make the nullclines (8) and (9) intersect at the desired point (12). Specifically, setting $\bar{D}_{12} := \bar{D}_1 + \bar{D}_2$ by using (8) and (10) we obtain

$$\bar{D}_{12} = \frac{\mu_1^*(s_{\rm in} - OD_{\rm d})}{(s_{\rm in} - OD_{\rm d} - k_1)}, \quad (13)$$

Moreover, by using (9) and (12) we get

$$\bar{D}_2 = r_{\rm d} \frac{OD_{\rm d}}{1 + r_{\rm d}} \cdot \frac{\bar{D}_{12} - \mu_2(s_{\rm in} - OD_{\rm d})}{\bar{x}_2^0}, \quad (14)$$

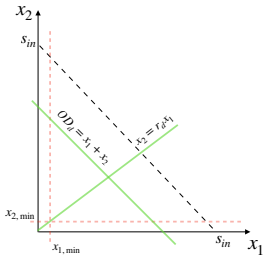

Fig. 2. Graphical representation of the control objective. The green solid lines represent the sets where $x_1 + x_2 = OD_{\mathrm{d}}$ and $x_2 = r_{\mathrm{d}} x_1$. The black dashed line delimits the invariant set $\mathcal{S}_r$. Finally, the orange dashed lines indicate the safety bounds for each species (i.e. $x_{1,\min}$, $x_{2,\min}$).

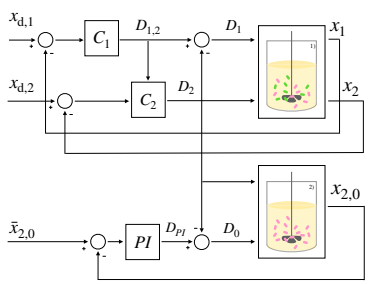

Fig. 3. Block diagram of the closed-loop control architecture. Two switching controllers, C_1 and C_2, regulate the concentrations of the biomasses x_1 and x_2 in chamber 1 to the desired levels $x_{\mathrm{d},1}$ and $x_{\mathrm{d},2}$, respectively. The control input D_0 regulating x_2^0 in chamber 2 to the desired level $\bar{x}_2^0$ is computed by a PI controller with a feedforward disturbance rejection.

where the steady-state value $\bar{x}_2^0$ in the reservoir can be reached by means of the control input

$$\bar{D}_0 = \mu_2(s_{\mathrm{in}} - \bar{x}_2^0) - \bar{D}_2, \tag{15}$$

obtained from setting the first term in (5) to zero. Obviously, we also have that $\bar{D}_1 = \bar{D}_{12} - \bar{D}_2$. Although this feedforward control action is very simple and solves the control problem in nominal conditions, as we will see later in Sec. VI, it does neither guarantee robustness to perturbation nor fast convergence.

V. Closed-Loop Control

In biological applications robustness is as important as precision in the regulation and open-loop strategies cannot often reject external perturbations and uncertainties in the model parameters. Therefore, we propose next a closed-loop switching controller that globally guarantees regulation of the desired density and composition.

This controller is designed under the assumption that the substrate is abundant, allowing both strains to grow at their maximum rate. Formally, under the assumption that the substrate s is abundant, i.e. $k_i \ll s$, $i = 1, 2$, the Monod's growth functions (4) can be approximated by their limit value, that is, $\mu_i(s) \approx \mu_i^*$. Hence, the reduced model (6) can be further simplified to:

$$\begin{cases} \dot{x}_1 = \mu_1^* x_1 - D_{12} x_1 \\ \dot{x}_2 = \mu_2^* x_2 - D_{12} x_2 + D_2 x_2^0 \end{cases}, \tag{16}$$

where $D_{12} := D_1 + D_2$ and the time dependence of the inputs is omitted to simplify the notation. System (16) has a unique equilibrium point

$$x_E = \left(0, \frac{D_2 x_2^0}{D_{12} - \mu_2^*}\right), \tag{17}$$

which is in the positive quadrant if $D_{12} > \mu_2^*$. The stability of x_E is dependent on the value of D_{12}. Specifically, if $\mu_2^* < D_{12} < \mu_1^*$, x_E is a saddle, with a positive eigenvalue associated to the eigenvector $\mathbf{u}_1 = (1, 0)^T$ and a negative eigenvalue associated to the eigenvector $\mathbf{u}_2 = (0, 1)^T$. This means that x_1 will diverge, while x_2 will asymptotically converge to $\frac{D_2 x_2^0}{D_{12} - \mu_2^*}$. Instead, if $D_{12} > \mu_1^*$, x_E is stable and all solutions in $\mathcal{S}_r$ will converge to it. Note that the stability of x_E depends only on D_{12} while its position on the x_2-axis can be moved by varying D_2.

Using the information on the position and stability of the equilibrium point (17), we can then design a switching controller that solves the control problem stated in Sec. III. Recalling that in system (16) the dynamics of x_1 is independent of the dynamics of x_2, we can decouple the design of the controller responsible for regulating the density of species 1, which we denote as C_1, from the controller taking the density of the species 2 to the desired value, namely C_2 (see Fig. 3). More precisely, we design the switching control law C_1 as:

$$D_{12} = \begin{cases} D_{12}^+ & \text{if } x_1 - x_{\mathrm{d},1} < 0 \\ D_{12}^- & \text{if } x_1 - x_{\mathrm{d},1} > 0 \end{cases}, \tag{18}$$

where $x_{\mathrm{d},i}$ is the i-th component of the set-point (12). Choosing $\mu_2^* < D_{12}^+ < \mu_1^*$, we guarantee that $\dot{x}_1 > 0$ when $x_1 < x_{\mathrm{d},1}$. Analogously, choosing $D_{12}^- > \mu_1^*$ ensures that $\dot{x}_1 < 0$ if $x_1 > x_{\mathrm{d},1}$. Hence, x_1 will converge to the desired value $x_{\mathrm{d},1}$.

The design of the controller C_2 can be decoupled from the design of C_1 by feeding it the value D_{12} as an input. Specifically, recalling (17) and considering that the dynamics on the x_2 component is always stable when $D_{12} > \mu_2^*$, we choose the switching controller C_2 as:

$$D_2 = \begin{cases} D_2^+ & \text{if } x_2 - x_{\mathrm{d},2} < 0 \\ D_2^- & \text{if } x_2 - x_{\mathrm{d},2} > 0 \end{cases}. \tag{19}$$

Choosing $\frac{x_{\mathrm{d},2}(D_{12} - \mu_2^*)}{x_2^0} < D_2^+ < D_{12}$ ensures that $\dot{x}_2 > 0$ if $x_2 < x_{\mathrm{d},2}$. Analogously, if we set $D_2^- < \frac{x_{\mathrm{d},2}(D_{12} - \mu_2^*)}{\bar{x}_2^0}$, $\dot{x}_2 < 0$ when $x_2 > x_{\mathrm{d},2}$. Therefore, x_2 will be converging towards $x_{\mathrm{d},2}$. Notice that a condition required for the controller to be realizable is that $\frac{x_{\mathrm{d},2}(D_{12} - \mu_2^*)}{x_2^0} < D_{12}$, which is verified if $x_{\mathrm{d},2} < x_2^0$.

The controller implemented in the reservoir (chamber 2) to regulate x_2^0 is a PI controller with a disturbance compensation. Specifically, the dilution rate D_0 in (5) is chosen as:

$$D_0 = D_{PI} - D_2, \tag{20}$$

where D_{PI} is an action computed using the same proportional-integral controller presented in [12] for the

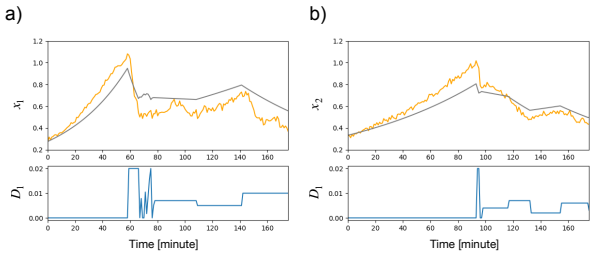

Fig. 4. Comparison between model predictions and the experimental data obtained from open-loop characterization experiments conducted using the Chi.Bio reactor. Two different *E. coli* strains implementing genetic toggle switches from [16] (panel a) and [17] (panel b) were used in the experiments. The top panels depict the temporal evolution of the biomass in the *in vivo* experiment (orange) and in the numerical simulation (gray). The bottom panels show the inputs applied to the bioreactors. The experimental data are collected using a single reactor (i.e. setting $D_0 = D_2 = 0$).

regulation of the turbidity. This controller ensures that the density of species 2 in the reservoir x_2^0 is regulated and maintained at the desired value $\bar{x}_2^0$.

VI. In silico validation

We validated the designed controllers through an exhaustive numerical simulation campaign to assess the performance and robustness of both the open-loop and the closed-loop control architectures. Specifically, we simulated the experimental platform shown in Fig. 1 implemented using two Chi.Bio reactors [12] and including the technological constraints imposed by the experimental platform. Each reactor measures the density of the biomasses grown within every minute by measuring the turbidity of the liquid (i.e. the optical density) and updates the duty-cycle of the peristaltic pumps that dilute the cultures with fresh media. Moreover, the dilution rates are saturated to 0.02 for safety reasons. In all control experiments we set the references as $OD_{\mathrm{d}} = 0.7$ and $r_{\mathrm{d}} = 1$.

A. Model parametrization

For the identification of the parameters in system (6), we conducted open-loop characterization experiments using the commercially available reactor Chi.Bio [12]. Specifically, we characterized the growth dynamics of two *E. coli* strains implementing two different implementations of a genetic toggle switch, presented in [16] and [17], respectively. In each experiment, using a single Chi.Bio reactor, we grew a single strain in LB media supplemented with $50\,\mu g/\mu L$ kanamycin and $1\,mM$ isopropyl β-D-1-thiogalactopyranoside (IPTG), at $37°C$, shaking at half the maximum speed available on the platform. During these experiments, the culture was diluted using the maximum available dilution rate ($0.02\,mL/s$) until the optical density dropped below 0.3. Then, cells underwent a recovery phase where the dilution rate was kept close to zero for 60 minutes. Finally, the cells' growth was excited changing the dilution rates every 15 to 30 minutes for 1 hour.

Using Genetic Algorithm (GA) optimization (as implemented in [18]), we estimated the growth parameters for each strain to be: $\mu_1^* = 0.026$, $\mu_2^* = 0.013$, $k_1 = 20.32$, $k_2 = 31.25$, and $s_{\mathrm{in}} = 88.75$. The range for each parameter

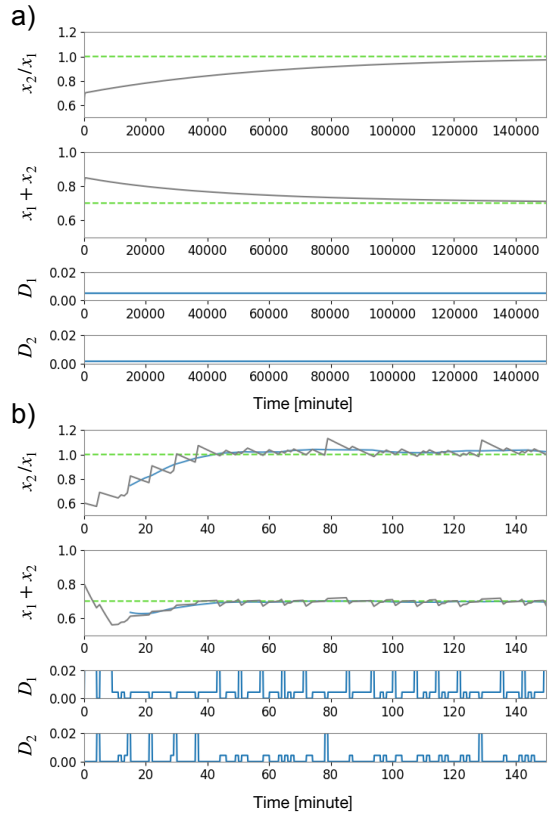

Fig. 5. *In silico* validation of the open-loop (a) and closed-loop (b) control strategies. The top panels show the evolution in time of x_2/x_1 and x_1+x_2, depicted as gray solid lines, together with the reference values (dashed green lines) and, for those in (b), the average trajectory over a time window of 30 minutes (blue solid line). The reference values are set as $OD_{\mathrm{d}} = 0.7$ and $r_{\mathrm{d}} = 1$. The bottom panels show the inputs administered to the first chamber.

were specified as follows: $[0.001, 0.05]$ for μ_1^*, μ_2^*, $[0.01, 100]$ for k_1, k_2, $[1, 100]$ for s_{in}. The total number of iterations was 200, and the initial population of the GA algorithm was set to be 150 individuals. In Fig. 4 the model's predictions are depicted alongside the experimental data, demonstrating its ability to capture quantitatively the growth dynamics of the microbial species under varying conditions. The quality of the predictions was quantified using the Root Mean Squared Error (RMSE), which proved to be low for the estimation of both populations' trajectories (i.e. RMSE $= 1.69$ for species 1 and RMSE $= 1.14$ for species 2).

B. Control validation

We simulated model (1)-(2) under the open-loop control action (with dilution rates equal to $D_1 = 0.016$, $D_2 = 0.0051$, $D_0 = 0.0044$, computed as described in Sec. IV), including also the technological constraints described above, observing that asymptotically the desired density and configuration were reached (see Fig. 5.a). However, the convergence time was excessively long, namely taking $97 \cdot 10^3$ min and $116 \cdot 10^3$ min to reach the desired optical density and ratio, respectively, rendering it unfeasible for *in vivo* implementation.

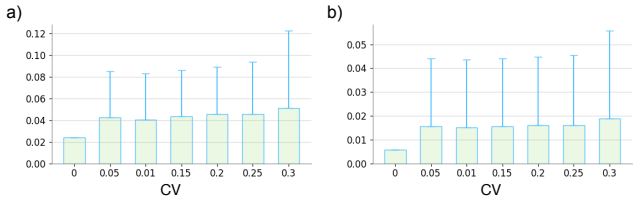

Fig. 6. Robustness analysis. Mean (bar height) and standard deviation (whisker) of $\bar{e}_r$ (panel a) and $\bar{e}_{OD}$ (panel b), for increasing value of the coefficient of variation CV. Each bar is obtained by averaging 100 simulations each computed with different values of parameters $(\mu_1^*, \mu_2^*, k_1, k_2)$.

Instead, as shown in Fig. 5.b) the switching control strategy developed in Sec. V was able to guarantee a much faster settling time (at 5%), namely, 32.5 min and 29.8 min for the optical density and the ratio between the two species, respectively, at the cost of a relatively small residual error at steady state. We quantified the relative residual errors by evaluating the average deviation from the desired values in the last 60 minutes of the experiments, that is, $\bar{e}_r = |(\bar{r} - r_{\mathrm{d}})/r_{\mathrm{d}}|$, where $\bar{r} = 1/60 \cdot \int_{t_f-60}^{t_f} (x_2(\tau)/x_1(\tau))d\tau$, where $t_f = 150\,\mathrm{min}$, and similarly for $\bar{e}_{OD}$, obtaining 0.024 and 0.0058, respectively.

Finally, we assessed the robustness of the proposed switched controller against variations in the parameters of the growth functions $\mu_i(s)$, $i = 1, 2$. Specifically, the values of the parameters $(\mu_1^*, \mu_2^*, k_1, k_2)$ were randomly drawn from normal distributions, each centered on their nominal value, say η, with a standard deviation equal to $\sigma = CV \cdot \eta$, where CV is the coefficient of variation. For each value of CV, taken in the interval $[0.05, 0.3]$, we evaluated the mean and standard deviation of the residual errors $\bar{e}_{OD}$ and $\bar{e}_r$ (normalized by the error for CV = 0), over 100 simulations of the closed-loop system, each computed with different values of the parameters $(\mu_1^*, \mu_2^*, k_1, k_2)$. The results of this analysis, reported in Fig. 6, highlight that, even in the case of a consistent mismatch between the identified parameters and their true value ($CV = 30\%$), the average steady-state residual errors stay below 0.05 for the ratio and 0.02 for the OD in absolute terms.

VII. CONCLUSIONS

We presented a two-reactor architecture for the control of the overall density and the composition a two strain microbial consortium. After analyzing the open-loop dynamics, we developed two *ad hoc* control strategies capable of solving the proposed control problem and validated them numerically using parameters identified with experimental data that have been acquired through a Chi.Bio reactor.

Our architecture enables long-term coexistence within a microbial consortium without requiring to engineer any additional circuit within the cells. This would enable the simultaneous growth of populations embedding different genetic circuits and even populations of different species (e.g. bacteria and yeasts), paving the way for the realization of stable multicellular consortia for the production of medicines, biofuels, and protein complexes [19].

We set up a prototype of the proposed experimental architecture represented in Fig. 1, comprising two Chi.Bio reactors. We are currently conducting *in vivo* experiments to validate the controllers presented here. The results of these experiments will be the subject of future work.

REFERENCES

[1] C. Zuñiga, L. Zaramela, and K. Zengler, "Elucidation of complexity and prediction of interactions in microbial communities," *Microbial Biotechnology*, vol. 10, no. 6, pp. 1500–1522, 2017.

[2] K. Zhou, K. Qiao, S. Edgar, and G. Stephanopoulos, "Distributing a metabolic pathway among a microbial consortium enhances production of natural products," *Nature Biotechnology*, vol. 33, no. 4, pp. 377–383, 2015.

[3] K. Brenner, L. You, and F. H. Arnold, "Engineering microbial consortia: a new frontier in synthetic biology," *Trends in Biotechnology*, vol. 26, no. 9, pp. 483–489, 2008.

[4] Y. Su, C. Liu, H. Fang, and D. Zhang, "Bacillus subtilis: a universal cell factory for industry, agriculture, biomaterials and medicine," *Microbial cell factories*, vol. 19, no. 1, pp. 1–12, 2020.

[5] J. J. Hug, D. Krug, and R. Müller, "Bacteria as genetically programmable producers of bioactive natural products," *Nature Reviews Chemistry*, vol. 4, no. 4, pp. 172–193, 2020.

[6] Y. Choi, T. J. Park, D. C. Lee, and S. Y. Lee, "Recombinant Escherichia coli as a biofactory for various single-and multi-element nanomaterials," *Proceedings of the National Academy of Sciences*, vol. 115, no. 23, pp. 5944–5949, 2018.

[7] T. A. Lee and H. Steel, "Cybergenetic control of microbial community composition," *Frontiers in Bioengineering and Biotechnology*, vol. 10, p. 1873, 2022.

[8] N. J. Treloar, A. J. Fedorec, B. Ingalls, and C. P. Barnes, "Deep reinforcement learning for the control of microbial co-cultures in bioreactors," *PLoS Computational Biology*, vol. 16, no. 4, p. e1007783, 2020.

[9] D. Fiore, F. Della Rossa, A. Guarino, and M. di Bernardo, "Feedback ratiometric control of two microbial populations in a single chemostat," *IEEE Control Systems Letters*, vol. 6, pp. 800–805, 2021.

[10] F.-Z. Tani *et al.*, "A hybrid control against species invasion in the chemostat," in *Proc. of the IEEE Conference on Decision and Control*, 2019, pp. 2814–2819.

[11] R. A. Armstrong and R. McGehee, "Competitive exclusion," *The American Naturalist*, vol. 115, no. 2, pp. 151–170, 1980.

[12] H. Steel, R. Habgood, C. Kelly, and A. Papachristodoulou, "Chi. Bio: An open-source automated experimental platform for biological science research," *BioRxiv*, p. 796516, 2019.

[13] J. Monod, "The growth of bacterial cultures," *Annual Review of Microbiology*, vol. 3, no. 1, pp. 371–394, 1949.

[14] P. De Leenheer and H. Smith, "Feedback control for chemostat models," *Journal of Mathematical Biology*, vol. 46, no. 1, pp. 48–70, 2003.

[15] H. L. Smith and P. Waltman, *The theory of the chemostat: dynamics of microbial competition*. Cambridge University Press, 1995.

[16] T. S. Gardner, C. R. Cantor, and J. J. Collins, "Construction of a genetic toggle switch in Escherichia coli," *Nature*, vol. 403, no. 6767, pp. 339–342, 2000.

[17] J.-B. Lugagne, S. Sosa Carrillo, M. Kirch, A. Köhler, G. Batt, and P. Hersen, "Balancing a genetic toggle switch by real-time feedback control and periodic forcing," *Nature Communications*, vol. 8, no. 1, p. 1671, 2017.

[18] M. J. Kochenderfer and T. A. Wheeler, *Algorithms for optimization*. Mit Press, 2019.

[19] N. S. McCarty and R. Ledesma-Amaro, "Synthetic biology tools to engineer microbial communities for biotechnology," *Trends in biotechnology*, vol. 37, no. 2, pp. 181–197, 2019.